HHS Public Access

Author manuscript

Biochem Biophys Res Commun. Author manuscript; available in PMC 2024 April 23.

Published in final edited form as:

Biochem Biophys Res Commun. 2020 November 26; 533(1): 168–174. doi:10.1016/j.bbrc.2020.08.010.

Pathogenic mutations perturb calmodulin regulation of $Na_v1.8$ channel

Liang Hong[a,*], **Meihong Zhang**[a], **Arvind Sridhar**[a], **Dawood Darbar**[a,b,c,**]

[a]Department of Medicine, University of Illinois at Chicago, Chicago, IL, USA

[b]Department of Pharmacology, University of Illinois at Chicago, Chicago, IL, USA

[c]Jesse Brown Veterans Administration, Chicago, IL, USA

Abstract

The voltage-gated sodium channels play a key role in the generation and propagation of the cardiac action potential. Emerging data indicate that the $Na_v1.8$ channel, encoded by the SCN10A gene, is a modulator of cardiac conduction and variation in the gene has been associated with arrhythmias such as atrial fibrillation (AF) and Brugada syndrome (BrS). The voltage gated sodium channels contain a calmodulin (CaM)-binding IQ domain involved in channel slow inactivation, we here investigated the role of CaM regulation of $Na_v1.8$ channel function, and showed that CaM enhanced slow inactivation of the $Na_v1.8$ channel and hyperpolarized steady-state inactivation curve of sodium currents. The effects of CaM on the channel gating were disrupted in the $Na_v1.8$ channel truncated IQ domain. We studied $Na_v1.8$ IQ domain mutations associated with AF and BrS, and found that a BrS-linked mutation (R1863Q) reduced the CaM-induced hyperpolarization shift, AF-linked mutations (R1869C and R1869G) disrupted CaM-induced enhanced inactivation, and effects of CaM on both development and recovery from slow inactivation were attenuated in all pathogenic mutations. Our findings indicate a role of CaM in the regulation of $Na_v1.8$ channel function in cardiac arrhythmias.

Keywords

$Na_v1.8$; Calmodulin; Voltage-gated sodium channel; Arrhythmia

1. Introduction

An important property of voltage-gated sodium channels is inactivation which prevents reopening of the channel until complete recovery thereby preventing action potential firing [1]. The voltage gated sodium channels contain a calmodulin (CaM)-binding IQ

*Corresponding author. Department of Medicine, University of Illinois at Chicago, Chicago, IL, 60612, USA., hong2004@uic.edu (L. Hong). **Corresponding author. Department of Medicine, University of Illinois at Chicago, Chicago, IL, 60612, USA., darbar@uic.edu (D. Darbar).

Declaration of competing interests

The authors declare that they have no known competing financial interests or personal relationships that could have appeared to influence the work reported in this paper.

Appendix A. Supplementary data

Supplementary data to this article can be found online at https://doi.org/10.1016/j.bbrc.2020.08.010.

motif important for channel inactivation [2,3]. Studies have shown that disease-associated mutations in the sodium channel IQ domain gave rise to arrhythmias, epilepsy, and autism [4–8]. The $Na_v1.5$-A1924T mutation, identified in patients with Brugada Syndrome, was shown to disrupt CaM binding and eliminate CaM-dependent slow inactivation, and alter $Na_v1.5$ channel in a manner characteristic of the Brugada syndrome [2], a similar mechanism has been described in another IQ domain mutation ($Na_v1.5$-R1919C) in patients with the Long QT Syndrome Type 3 (LQT3) [4]. In $Na_v1.2$ channel, the $Na_v1.2$-R1902C mutation linked with autism was shown to disrupt the interaction between $Na_v1.2$ channel and CaM, producing gain-of-function shift in the kinetics of $Na_v1.2$ channel activation and steady-state inactivation [9].

Recently, genetic research demonstrated that $Na_v1.8$ channel, encoded by *SCN10A* gene, as a modulator of cardiac conduction [10]. $Na_v1.8$ channel has been identified in cardiomyocytes and intracardiac neurons with a contribution to cardiac repolarization [11,12]. Studies have identified a number of $Na_v1.8$ mutations linked with risk of atrial fibrillation (AF) and Brugada syndrome (BrS) [13–15]. The $Na_v1.8$-R1863Q mutation was identified in a patient diagnosed with BrS [13], $Na_v1.8$-R1869G mutation was associated with persistent AF [14], and $Na_v1.8$-R1869C mutation was identified in an index case with both AF and BrS [15]. These mutations all are located in the highly conserved IQ domain, highlighting their possible roles in regulation interaction CaM and $Na_v1.8$ channel.

Previous studies have shown mutations in the $Na_v1.5$ channel IQ domain perturbed CaM-induced slow inactivation with a weakening of the $Na_v1.5$-CaM interaction [2,4]. Although $Na_v1.8$ contributes to regulation of cardiac function and shares high sequence homology with $Na_v1.5$ channel, it remains to unclear if CaM modulation of $Na_v1.8$ channel also plays a role in arrhythmogenesis. Here, we sought to examine the role of CaM regulation of $Na_v1.8$ channel function and how CaM modulates $Na_v1.8$ sodium channel gating, whether and how AF and BrS-linked mutations affect interaction between CaM and $Na_v1.8$ channel.

2. Material and methods

$Na_v1.8$ transfection and cell culture.

Details of cell culture and $Na_v1.8$ transfections are available in the Supplementary material.

2.1. Electrophysiological measurements and analysis

Patch-clamp measurements were performed in a whole-cell configuration using an Axopatch 200B amplifier controlled by pClamp 10 software through an Axon Digidata 1440A system (all from Molecular Devices, LLC, Sunnyvale, CA, USA).

To test steady-state inactivation, currents were elicited to −10 mV following prepulses ranging between −140 and 0 mV in 10 mV steps for 500 m s. Development and recovery of slow inactivation were assessed using a two-pulse voltage clamp protocol [16]. To investigate development of inactivation, the currents were assayed by varying the duration of a conditioning pulse *P1* (5–2000 m s) to 10 mV followed by a return to −120 mV for 20 m s followed by a 100 m s test pulse *P2* to −10 mV. The recovery of inactivation for the sodium

currents was assessed using protocol with a conditioning pulse duration of 1000 m s (*P1*) and a test pulse of 200 m s (*P2*) to −10 mV with varying rest intervals from 5 to 2000 ms at −120 mV. The current densities were calculated according to whole-cell current amplitude and capacitance values obtained from the amplifier following electronic subtraction of the capacitive transients [17]. Whole-cell currents were acquired at a sampling interval of 10 kHz and filtered at 1 kHz. Pulse generation and data collection were done with Clampex 10.1 [18]. All measurements were performed at 22 ± 3 °C.

Steady-state inactivation was fitted by the *Boltzmann* equation as described previously [19]: $I/I_{max} = 1/(1 + exp(V - V_{1/2})/k)$, where I/I_{max} is the relative conductance normalized by the maximal conductance, $V_{1/2}$ is half-maximal inactivation, V is test pulse, and k is the *Boltzmann* coefficient. Dose-responses relations were determined by plotting the $V_{1/2}$ at each CaM concentration, and were fitted by the Hill equation as described previously [20]: $\%_i = \%_{i,max}[B]^h/(EC_{50}^h + [B]^h)$, where $\%_{i,max}$ is the maximal percentage of $V_{1/2}$ generated by B, which is CaM here, h is the Hill coefficient and EC_{50} is the concentration of the CaM required for 50% $V_{1/2}$. Exponential functions of the form: $y = y0 + A\ (1 - exp\ [-t/\tau])$ were fitted to development curves to determine time constant (τ_{dev}), where $y0$ is the offset and A is amplitude. Exponential functions of the form: $y = A1\ (1 - exp\ [-t/\tau 1) + A2\ (1 - exp[-t/\tau 2])$ were fitted to recovery curves to determine time constants ($\tau_{rec,f}$, $\tau_{rec,s}$), $A1$ and $A2$ are the fractions of fast and slow inactivating components, and $\tau 1$ and $\tau 2$ are their time constants $\tau_{rec,f}$ and $\tau_{rec,s}$ respectively.

2.2. Solutions and drugs

$Na_V1.8$ currents in transiently transfected ND7/23 cells were recorded using an external solution that contained: 145 mM NaCl, 4 mM KCl, 1.8 mM $CaCl_2$, 1 mM $MgCl_2$, 10 mM HEPES, and 10 mM glucose, adjusted to pH 7.4 with NaOH. The intracellular solution contained 100 mM CsF, 10 mM NaF, 20 mM CsCl, 5 mM EGTA, 3.7 mM $CaCl_2$, and 10 mM HEPES, adjusted to pH 7.35 with CsOH [21]. The CaM and CaM inhibitory peptide 290–309 (Enzo Life Sciences, Inc., Farmingdale, USA) were added to the pipette solution to final concentrations. Endogenous tetrodotoxin (TTX)-sensitive sodium currents in ND7/23 cells were eliminated with 200 nM TTX as previously reported [14].

2.3. Data and statistical analysis

All data are presented as the means ± S.E.M. Significance between means was determined by Student's t-test or analysis of variance (ANOVA) as appropriate. Electrophysiological parameters ($V_{1/2}$, time constants τ_{dev}, $\tau_{rec,f}$, $\tau_{rec,s}$) were determined from each individual cell and then used for comparison with either *t*-test or ANOVA. For each group cell, the data were collected from 3 to 4 independent transfections, 2–3 sodium currents were recorded in each independent culture. Paired *t*-test was used for comparison of parameters between groups with or without CaM. ANOVA was conducted for identifying statistically significant differences among multiple groups. $P < 0.05$ was considered to indicate a statistically significant difference.

3. Results

3.1. Pathogenic mutations associated with AF and BrS in the $Na_v1.8$ channel IQ domain

A number of $Na_v1.8$ mutations within the IQ domain have recently been linked with cardiac arrhythmias. One clinical research reported an $Na_v1.8$-R1863Q mutation in a patient with Brugada syndrome (BrS), the patient's electrocardiography presented a significant coved-type ST elevation with induced ventricular fibrillation [13]. The other mutation $Na_v1.8$-R1869C was identified in an index case with both atrial fibrillation (AF) and BrS. This mutation was found in two AF probands with BrS phenotypes [15]. Our group identified $Na_v1.8$ mutation R1869G within the IQ domain that co-segregated with familial AF. The proband in the family presented with symptomatic AF, and this mutation was not presented in unaffected familiar members [14]. As three mutations are localized to the IQ domain of the $Na_v1.8$ channel (Fig. 1), we investigated effects of CaM on $Na_v1.8$ channel and the interaction between CaM and $Na_v1.8$ IQ domain.

3.2. Effects of CaM on $Na_v1.8$ channel

We studied whole-cell $Na_v1.8$ currents and observed that CaM (10 μM) caused a hyperpolarizing shift (~17 mV) in the steady-state inactivation of the $Na_v1.8$ channel (−72.0 ± 2.8 mV *vs* −55.2 ± 2.6 mV, n = 8 cells in each group) without significantly affecting its activation curve (−16.7 ± 2.9 mV *vs* −15.3 ± 3.2 mV, n = 6 in each group) (Fig. 2A–B and Table S2–S3). In addition, CaM decreased the time constant for development (τ_{dev}) (554 ± 17 m s *vs* 735 ± 33 m s, n = 8), and delay fast recovery time constant $\tau_{rec,f}$ (5.9 ± 0.3 m s *vs* 3.7 ± 0.4 m s, n = 8) and slow recovery time constant $\tau_{rec,s}$ (86.2 ± 8.7 m s *vs* 63.7 ± 6.7 m s, n = 8), suggesting that it enhanced development and slowed recovery from inactivated states (Fig. 2C–D and Table S4). The addition of 290–309, a CaM inhibitory peptide, did not significantly affect inactivation of the channel; however, 290–309 plus CaM reduced the hyperpolarizing shift induced by CaM alone −60.3 ± 4.4 mV *vs* −72.0 ± 2.8 mV) (Fig. S1 and Table S2). We further determined if the steady-state inactivation hyperpolarization shift was dose dependent. Raising intracellular CaM concentrations from 1 to 50 μM caused a leftward shift in availability. The membrane potential at which 50% of the channels were available to open ($V_{1/2}$) was: −60.8 ± 3.9 mV, −65. 2 ± 3.1 mV, −72.0 ± 2.8 mV, −78.5 ± 2.9 mV, −80.4 ± 3.4 mV for 1, 5, 10, 20, and 50 μM respectively (Fig. S2 and Table S2), a dose-response curve fitted to the $V_{1/2}$ data yielded an EC_{50} value with CaM of 9.2 μM. Collectively, these results show that CaM significantly enhanced slow inactivation of the $Na_v1.8$ channel and reduced channel availability.

3.3. CaM modulates $Na_v1.8$ channel gating through the IQ domain

Like other voltage gated sodium channels, $Na_v1.8$ channel contains a CaM-binding IQ domain important for channel inactivation. To evaluate functional effects of $Na_v1.8$ channel IQ domain on the CaM binding, we generated two truncated constructs ($S1835_{stop}$ and $G1893_{stop}$) and a mutation IQ/AA (substitution of two conserved residues isoleucine and glutamine with double alanine). The IQ/AA mutation channel has been reported to disrupt CaM binding to the IQ domain of sodium channels [22]. The truncated $S1835_{stop}$ channel does not contain IQ domain, and $G1893_{stop}$ channel contained an intact IQ domain

(Fig. 3A). We found that CaM-mediated regulation of $Na_v1.8$ channel was abrogated in IQ/AA mutation and $S1835_{stop}$ channels (Fig. 3 and Table S2–S3). The CaM-induced hyperpolarizing shift ($\Delta V_{1/2}$) in the IQ/AA mutation and $S1835_{stop}$ channel were 3.3 ± 0.5 mV and 0.3 ± 1.0 mV, compared with WT channel 16.9 ± 0.7 mV. In contrast, truncated $G1893_{stop}$ channel containing the intact IQ domain restored the hyperpolarizing shift in channel inactivation evoked by CaM ($\Delta V_{1/2}$ is 12.8 ± 0.6 mV), compared with IQ/AA ($\Delta V_{1/2}$ is 3.3 ± 0.5 mV) and $S1835_{stop}$ ($\Delta V_{1/2}$ is 0.3 ± 1.0 mV) (Fig. 3G and Table S3). These results support CaM regulation of $Na_v1.8$ channel function by binding to the IQ domain.

3.4. The AF and BrS-linked $Na_v1.8$ mutations affect CaM interacting with $Na_v1.8$ channel

As a number of AF- and BrS-associated $Na_v1.8$ mutations are located in the IQ domain of the channel (Fig. 1) [13–15], we assessed their role in regulating the interaction between CaM and the channel. We observed that CaM produced a hyperpolarizing shift in the $V_{1/2}$ of steady-state inactivation in the R1863Q mutation (−66.8 ± 2.2 mV *vs* −59.4 ± 2.2 mV, n = 8) (Fig. 4A–C, J and Table S2); however, the extent of $V_{1/2}$ shift generated by CaM ($\Delta V_{1/2}$) in R1863Q was markedly decreased compared with WT channel ($\Delta V_{1/2}$ is 7.4 ± 0.3 mV *vs* 16.9 ± 0.7 mV) (Fig. 4K and Table S3). Moreover, the addition of CaM to the R1869C and R1869G mutations failed to hyperpolarize the channels (−49.2 ± 3.4 mV *vs* −46.1 ± 2.1 mV and −61.4 ± 2.7 mV *vs* −60.1 ± 3.3 mV, respectively) (Fig. 4D–J and Table S2), and no significant CaM-induced shifts ($\Delta V_{1/2}$ are 3.1 ± 1.3 mV and 0.9 ± 0.7 mV, respectively) were observed in the two mutations (Fig. 4K and Table S3). The three mutations altered time constants for development τ_{dev}, or for fast recovery $\tau_{rec,f}$ compared with WT $Na_v1.8$ channel to different extents (Figs. S3–S4 and Table S4–S5). The alterations of time constants τ_{dev} or $\tau_{rec,f}$ induced by CaM ($\Delta\tau_{dev}$ or $\Delta\tau_{rec,f}$) were all significantly attenuated in three mutations (Fig. S3E, Fig. S4E and Table S5), suggesting that $Na_v1.8$ IQ domain mutations perturb the interaction between CaM and the channel, and weaken CaM regulation of channel function.

4. Discussion

We determined the role of CaM in modulating $Na_v1.8$ channel gating, and showed that CaM regulated $Na_v1.8$ channel availability and enhanced steady-state inactivation by interacting with the IQ domain. AF and BrS-associated mutations within the IQ domain destabilized the CaM-induced binding and abrogated the hyperpolarization shift.

The voltage-gated sodium channels play crucial roles in the generation and propagation of the action potential. The family of sodium channels has nine members named $Na_v1.1$ through $Na_v1.9$, and $Na_v1.5$ is the predominant subtype sodium channel initiating cardiac action potential duration (APD) [23]. Increasing evidence suggests that another sodium channel $Na_v1.8$ influences cardiac conduction and plays an important role in the heart [10]. The cellular localization of $Na_v1.8$ within the heart is highly variable across cardiac chambers with enhanced expression in the conduction system, intracardiac neurons, and atrial cardiac tissue [11,12,23]. $Na_v1.8$ expressions were observed in human cardiac nerve fibres and cardiomyocytes isolated from the atrial appendage [24], and in intracardiac neurons in mouse [12]. Previous study has shown that CaM associated with $Na_v1.8$ in the dorsal root ganglion (DRG) neurons regulating frequency-dependent inhibition of

$Na_v1.8$ channel, supporting CaM is a functional partner of $Na_v1.8$ sodium [25]. Here we demonstrated CaM modulates $Na_v1.8$ function through its interaction with the IQ domain and showed CaM-mediated regulation was abrogated either in a mutation disrupting CaM binding or in a truncated channel without the IQ domain (Fig. 3).

All voltage-gated sodium channels contain a CaM-binding IQ domain important for channel inactivation [26]. It not only helps prevent reopening of the channel until recovery but also regulates the frequency of action potential firing and reduces the breakdown of ionic gradients and cell death [1]. Many regulatory partners and intracellular proteins affect sodium channel inactivation, and the significance of CaM and its interaction with the sodium channel IQ domain is highlighted because disease-associated mutations in the domain give rise to arrhythmias, epilepsy, and autism by interfering with the CaM-induced interaction [4–8].

A $Na_v1.5$ BrS mutation ($Na_v1.5$-A1924T) in the IQ domain inhibited CaM-induced slow inactivation with a predicted weakening of the $Na_v1.5$-CaM interaction [2]. A similar mechanism has been described in patients with the Long QT Syndrome Type 3 and BrS-causing $Na_v1.5$-R1919C mutation [4]. It should be noted that the $Na_v1.5$-R1919C corresponds to the $Na_v1.8$-R1869C (Fig. 1). We showed that the $Na_v1.8$-R1869C mutation associated with AF and BrS abrogated the effects of CaM on the channel, and CaM failed to hyperpolarize inactivation of the channel. In addition, a second AF-linked mutation at the same position R1869 ($Na_v1.8$-R1869G) generated a more severe phenotype with almost complete disruption of CaM-induced enhancement of inactivation (Fig. 4). Like $Na_v1.8$-R1869, $Na_v1.8$-R1863 is a highly conserved arginine in the IQ domain across the sodium channel family (Fig. 1), and these conserved positive residues have been proposed to couple with negative residues of CaM to form charge-charge interaction stabilizing CaM binding to the IQ domain [4,9]. We showed that $Na_v1.8$-R1863Q exhibited a reduced hyperpolarization shift mediated by CaM (Fig. 4K), which might be caused by the uncoupling of this charge-charge interaction, and this equivalent position mutation in $Na_v1.2$ (R1918H) was identified in a patient with febrile seizures and epilepsy [7].

Under physiological condition, CaM binding enhances slow inactivation of the cardiac sodium channel [1]. Perturbation of this gating process caused by cardiac sodium channel mutations generally reduce the channel availability [2]. As the cardiac sodium channel availability is crucial for the normal electrical activity of cardiomyocytes, gating defects can give rise to abnormal APD and increased susceptibility to arrhythmias. Previous studies have demonstrated that $Na_v1.8$ directly regulates cardiac conduction. In the current study, the mutations associated with BrS and AF destabilized the interaction of CaM with the channel IQ domain, attenuating CaM-mediated slow inactivation, and potentially limit the propensity for transient changes in intracellular CaM to trigger cardiac arrhythmias.

In summary, we showed that CaM interaction with the IQ domain of the $Na_v1.8$ channel plays an important role in controlling channel availability. Destabilization of the interaction between CaM and $Na_v1.8$ channel by pathologic mutations may be proarrhythmic and give rise to the electrophysiologic substrates underlying cardiac arrhythmias.

Supplementary Material

Refer to Web version on PubMed Central for supplementary material.

Acknowledgments

This work was supported by AHA Award 19CDA34630041 (to L.H.), and NIH R01 grants HL138737, HL150586 and T32 HL139439 (to D.D.).

References

[1]. Ulbricht W, Sodium channel inactivation: molecular determinants and modulation, Physiol. Rev. 85 (2005) 1271–1301, 10.1152/physrev.00024.2004. [PubMed: 16183913]

[2]. Tan HL, Kupershmidt S, Zhang R, Stepanovic S, Roden DM, Wilde AA, Anderson ME, Balser JR, A calcium sensor in the sodium channel modulates cardiac excitability, Nature 415 (2002) 442–447, 10.1038/415442a.

[3]. Ben-Johny M, Yang PS, Niu J, Yang W, Joshi-Mukherjee R, Yue DT, Conservation of Ca2+/calmodulin regulation across Na and Ca2+ channels, Cell 157 (2014) 1657–1670, 10.1016/j.cell.2014.04.035. [PubMed: 24949975]

[4]. Gabelli SB, Yoder JB, Tomaselli GF, Amzel LM, Calmodulin and Ca(2+) control of voltage gated Na(+) channels, Channels 10 (2016) 45–54, 10.1080/19336950.2015.1075677.

[5]. Wang C, Chung BC, Yan H, Wang HG, Lee SY, Pitt GS, Structural analyses of Ca(2)(+)/CaM interaction with NaV channel C-termini reveal mechanisms of calcium-dependent regulation, Nat. Commun. 5 (2014), 10.1038/ncomms5896, 4896.

[6]. Gabelli SB, Boto A, Kuhns VH, Bianchet MA, Farinelli F, Aripirala S, Yoder J, Jakoncic J, Tomaselli GF, Amzel LM, Regulation of the NaV1.5 cytoplasmic domain by calmodulin, Nat. Commun. 5 (2014), 10.1038/ncomms6126, 5126.

[7]. Haug K, Hallmann K, Rebstock J, Dullinger J, Muth S, Haverkamp F, Pfeiffer H, Rau B, Elger CE, Propping P, Heils A, The voltage-gated sodium channel gene SCN2A and idiopathic generalized epilepsy, Epilepsy Res. 47 (2001) 243–246.

[8]. Weiss LA, Escayg A, Kearney JA, Trudeau M, MacDonald BT, Mori M, Reichert J, Buxbaum JD, Meisler MH, Sodium channels SCN1A, SCN2A and SCN3A in familial autism, Mol. Psychiatr. 8 (2003) 186–194, 10.1038/sj.mp.4001241.

[9]. Pitt GS, Lee SY, Current view on regulation of voltage-gated sodium channels by calcium and auxiliary proteins, Protein Sci. 25 (2016) 1573–1584, 10.1002/pro.2960.

[10]. Chambers JC, Zhao J, Terracciano CM, Bezzina CR, Zhang W, Kaba R, Navaratnarajah M, Lotlikar A, Sehmi JS, Kooner MK, Deng G, Siedlecka U, Parasramka S, El-Hamamsy I, Wass MN, Dekker LR, de Jong JS, Sternberg MJ, McKenna W, Severs NJ, de Silva R, Wilde AA, Anand P, Yacoub M, Scott J, Elliott P, Wood JN, Kooner JS, Genetic variation in SCN10A influences cardiac conduction, Nat. Genet. 42 (2010) 149–152, 10.1038/ng.516.

[11]. Yang T, Atack TC, Stroud DM, Zhang W, Hall L, Roden DM, Blocking Scn10a channels in heart reduces late sodium current and is antiarrhythmic, Circ. Res. 111 (2012) 322–332, 10.1161/CIRCRESAHA.112.265173.

[12]. Verkerk AO, Remme CA, Schumacher CA, Scicluna BP, Wolswinkel R, de Jonge B, Bezzina CR, Veldkamp MW, Functional $Na_V1.8$ channels in intracardiac neurons: the link between SCN10A and cardiac electrophysiology, Circ. Res. 111 (2012) 333–343, 10.-1161/CIRCRESAHA.112.274035.

[13]. Fukuyama M, Ohno S, Makiyama T, Horie M, Novel SCN10A variants associated with Brugada syndrome, Europace 18 (2016) 905–911, 10.1093/europace/euv078.

[14]. Savio-Galimberti E, Weeke P, Muhammad R, Blair M, Ansari S, Short L, Atack TC, Kor K, Vanoye CG, Olesen MS, LuCamp T, Yang A.L. George Jr., Roden DM, Darbar D, SCN10A/$Na_V1.8$ modulation of peak and late sodium currents in patients with early onset atrial fibrillation, Cardiovasc. Res. 104 (2014) 355–363, 10.1093/cvr/cvu170.

[15]. Hu D, Barajas-Martinez H, Pfeiffer R, Dezi F, Pfeiffer J, Buch T, Betzenhauser MJ, Belardinelli L, Kahlig KM, Rajamani S, DeAntonio HJ, Myerburg RJ, Ito H, Deshmukh P, Marieb M, Nam GB, Bhatia A, Hasdemir C, Haissaguerre M, Veltmann C, Schimpf R, Borggrefe M, Viskin S, Antzelevitch C, Mutations in SCN10A are responsible for a large fraction of cases of Brugada syndrome, J. Am. Coll. Cardiol. 64 (2014) 66–79, 10.1016/j.jacc.2014.04.032.

[16]. Alkhalil A, Hong L, Nguitragool W, Desai SA, Voltage-dependent inactivation of the plasmodial surface anion channel via a cleavable cytoplasmic component, Biochim. Biophys. Acta 1818 (2012) 367–374, 10.1016/j.bbamem.2011.11.010.

[17]. Kim IH, Hevezi P, Varga C, Pathak MM, Hong L, Ta D, Tran CT, Zlotnik A, Soltesz I, Tombola F, Evidence for functional diversity between the voltage-gated proton channel Hv1 and its closest related protein HVRP1, PloS One 9 (2014), 10.1371/journal.pone.0105926e105926.

[18]. Pathak MM, Tran T, Hong L, Joos B, Morris CE, Tombola F, The Hv1 proton channel responds to mechanical stimuli, J. Gen. Physiol. 148 (2016) 405–418, 10.1085/jgp.201611672.

[19]. McCauley MD, Hong L, Sridhar A, Menon A, Perike S, Zhang M, da Silva IB, Yan J, Bonini MG, Ai X, Rehman J, Darbar D, ion channel and structural remodeling in obesity: mediated atrial fibrillation, Circ Arrhythm Electrophysiol, 2020, 10.1161/CIRCEP.120.008296.

[20]. Liu J, Liu D, Liu JJ, Zhao C, Yao S, Hong L, Blocking the $Na_V1.5$ channel using eicosapentaenoic acid reduces migration and proliferation of ovarian cancer cells, Int. J. Oncol. 53 (2018) 855–865, 10.3892/ijo.2018.4437.

[21]. Deschenes I, Neyroud N, DiSilvestre D, Marban E, Yue DT, Tomaselli GF, Isoform-specific modulation of voltage-gated Na(+) channels by calmodulin, Circ. Res. 90 (2002) E49–E57.

[22]. Biswas S, Deschenes I, Disilvestre D, Tian Y, Halperin VL, Tomaselli GF, Calmodulin regulation of $Na_V1.4$ current: role of binding to the carboxyl terminus, J. Gen. Physiol. 131 (2008) 197–209, 10.1085/jgp.200709863.

[23]. Zimmer T, Haufe V, Blechschmidt S, Voltage-gated sodium channels in the mammalian heart, Glob Cardiol Sci Pract 2014 (2014) 449–463, 10.5339/gcsp.2014.58.

[24]. Facer P, Punjabi PP, Abrari A, Kaba RA, Severs NJ, Chambers J, Kooner JS, Anand P, Localisation of SCN10A gene product Na(v)1.8 and novel pain-related ion channels in human heart, Int. Heart J. 52 (2011) 146–152.

[25]. Choi JS, Hudmon A, Waxman SG, Dib-Hajj SD, Calmodulin regulates current density and frequency-dependent inhibition of sodium channel $Na_V1.8$ in DRG neurons, J. Neurophysiol. 96 (2006) 97–108, 10.1152/jn.00854.2005.

[26]. Ben-Johny M, Dick IE, Sang L, Limpitikul WB, Kang PW, Niu J, Banerjee R, Yang W, Babich JS, Issa JB, Lee SR, Namkung H, Li J, Zhang M, Yang PS, Bazzazi H, Adams PJ, Joshi-Mukherjee R, Yue DN, Yue DT, Towards a unified theory of calmodulin regulation (calmodulation) of voltage-gated calcium and sodium channels, Curr. Mol. Pharmacol. 8 (2015) 188–205.

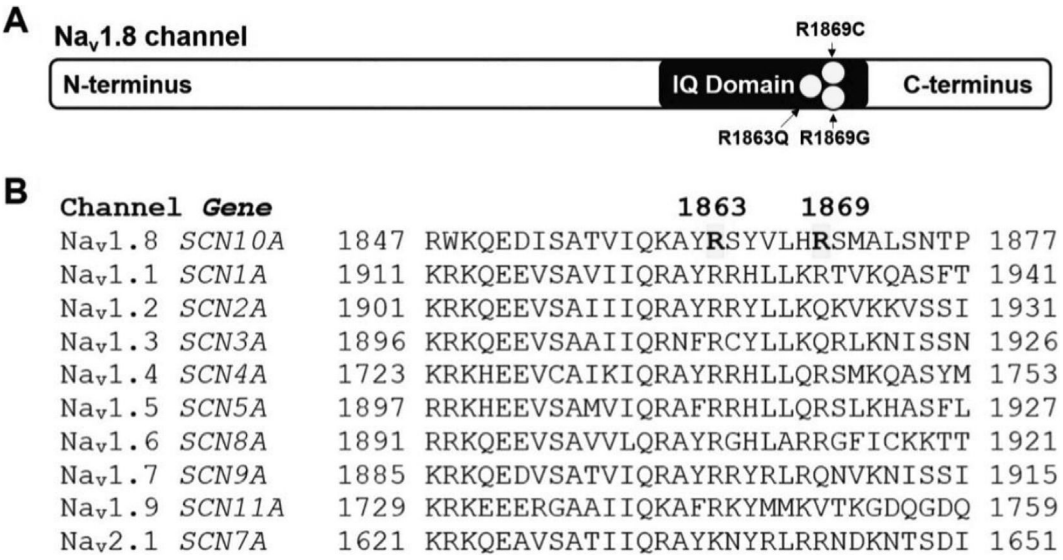

Fig. 1. Na$_v$1.8 mutations in the IQ domain associated with Brugada syndrome (BrS) and atrial fibrillation (AF).

(***A***) A schematic representation showing the structure of the Na$_v$1.8 channel. Pathogenic mutations are highlighted in yellow, the *N*- and *C*-terminus of the channel are shown with the IQ domain in black. (***B***) Alignment of voltage-gated sodium channel family IQ domain.

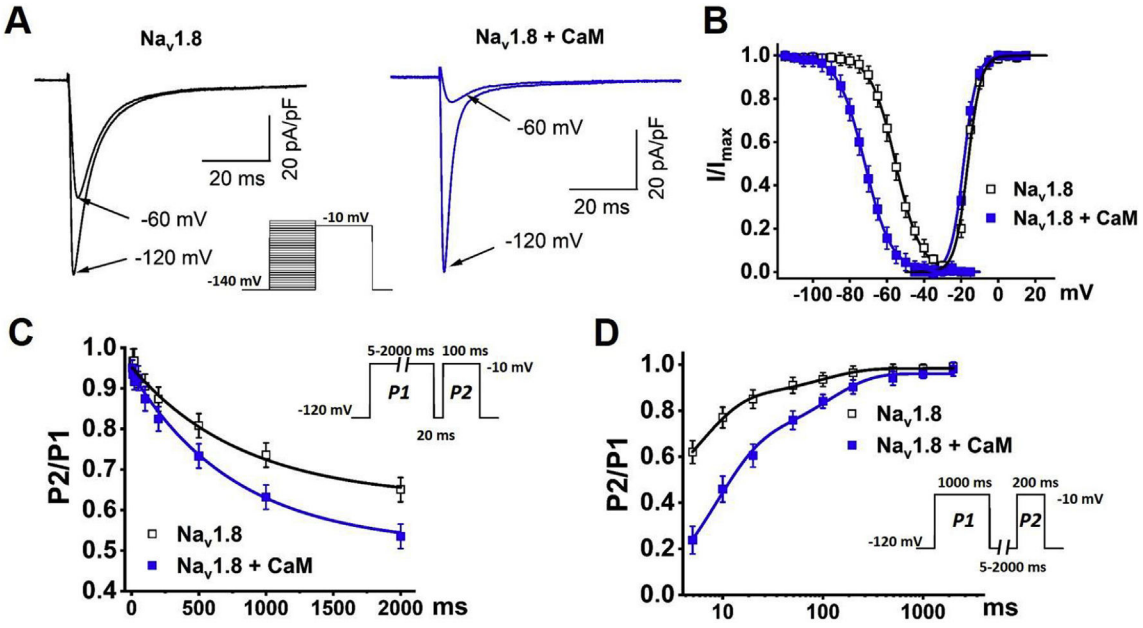

Fig. 2. Effects of CaM on steady-state inactivation of the Na$_v$1.8 channel.

(***A***) Two pulse protocol is used to measure steady-state inactivation, exemplar wild-type (WT) Na$_v$1.8 sodium currents without (left panel, black traces) and with CaM (10 μM; right panel, blue traces). Currents were elicited to −10 mV following prepulses ranging between −140 and 0 mV in 5 mV steps for 500 m s. (***B***) Steady-state activation and inactivation curves of Na$_v$1.8 sodium currents in the presence or absence of CaM. Curves are *Boltzmann* fits of the data points. (n = 8 cells; data are presented as the means ± SEM). (***C***) Development of inactivation for Na$_v$1.8 sodium currents in the presence or absence of CaM was assessed by varying the duration of a conditioning pulse *P1* (5–2000 m s) to −10 mV followed by a return to −120 mV for 20 m s followed by a 100 m s test pulse *P2* to −10 mV. (***D***) Recovery of inactivation for Na$_v$1.8 sodium currents in the presence or absence of CaM was assessed using insert protocol with a first pulse duration of 1000 m s (*P1*) and a second pulse of 200 m s (*P2*) to 10 mV with varying rest intervals from 5 to 2000 ms at −120 mV. Curves in (***C***) and (***D***) are exponential function fits of the data points, n = 8 cells in each group. (For interpretation of the references to colour in this figure legend, the reader is referred to the Web version of this article.)

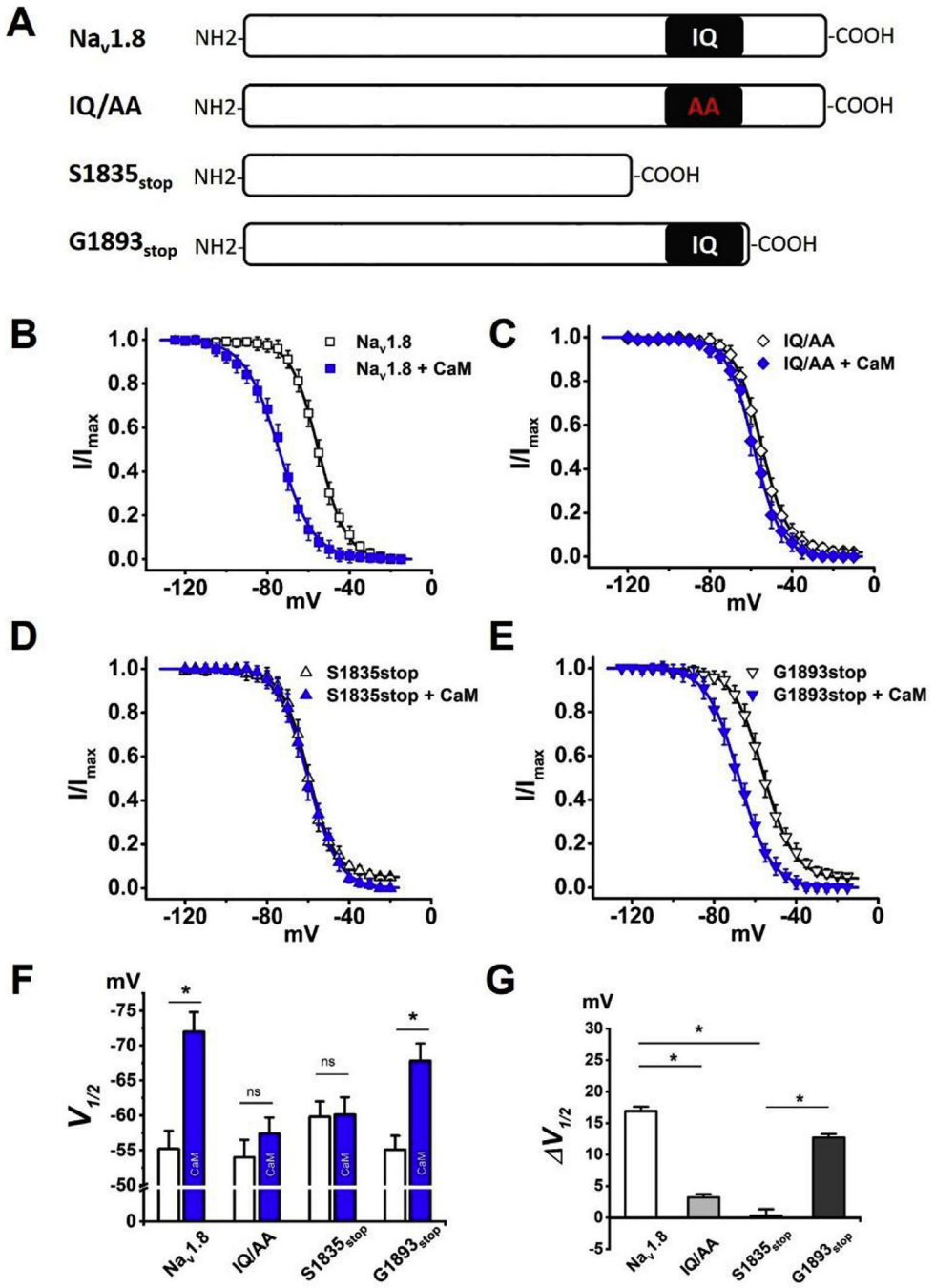

Fig. 3. CaM modulated Na$_v$1.8 channel gating through the IQ domain.

(***A***) Schematic representation of wild-type (WT) Na$_v$1.8, IQ mutation (IQ/AA), and *C*-terminus truncations (S1835$_{stop}$ and G1893$_{stop}$) of the Na$_v$1.8 channel. (**B**-**E**) Steady-state inactivation curves of WT Na$_v$1.8 (***B***) and mutated Na$_v$1.8 channels IQ/AA (***C***), S1835$_{stop}$ (***D***) and G1893$_{stop}$ (***E***) in the absence (black trace) and presence of CaM (blue trace; n = 6–7 cells in each group). Curves are *Boltzmann* fits of the data points. (***F***) Summary of $V_{1/2}$ of steady-state inactivation for WT and mutated Na$_v$1.8 channels in the presence or absence of CaM. $V_{1/2}$ s are assessed by *Boltzmann* fits from (***B***-***E***). (*$P < 0.05$; ns, not significant). (G)

Shifts of $V_{1/2}$ ($\Delta V_{1/2}$) of inactivation produced by CaM in WT and mutated $Na_V1.8$ channels. $\Delta V_{1/2}$ are assessed from (***F***) (*$P < 0.05$). (For interpretation of the references to colour in this figure legend, the reader is referred to the Web version of this article.)

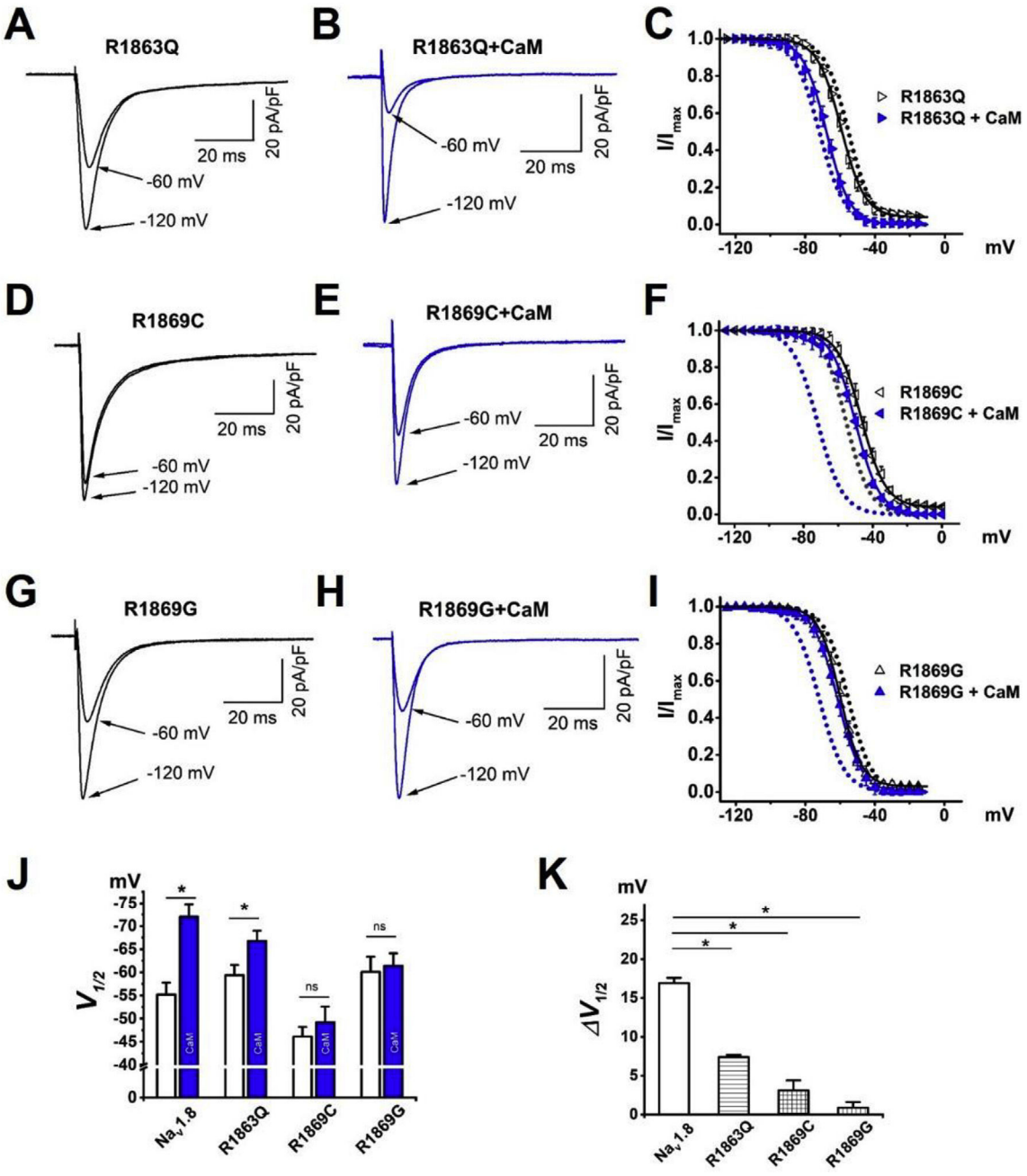

Fig. 4. The AF and BrS-linked mutations affect CaM regulation of steady-state inactivation of $Na_v1.8$ channel.

(**A-I**) Two pulse protocol is used to measure steady-state inactivation, exemplar R1863Q (***A***), R1863Q + CaM (***B***), R1869C (***D***), R1869C + CaM (***E***), R1869G (***G***), and R1869G + CaM (***H***). (***C***) Steady-state inactivation of R1863Q and R1863Q + CaM. (***F***) Steady-state inactivation of R1869C and R1869C + CaM. (***I***) Steady-state inactivation of R1869G and R1869G + CaM. The dashed lines represent WT $Na_v1.8$ (black dash curve) and WT $Na_v1.8$ + CaM (blue dash curve) in the panel (***C***), (***F***), and (***I***). n = 7–9 cells in each group. Curves are *Boltzmann* fits of the data points. (***J***) Summary of $V_{1/2}$ of steady-state inactivation for $Na_v1.8$ mutations in the presence or absence of CaM. (*$P < 0.05$; ns, not significant). (***K***)

Shifts of $V_{1/2}$ of inactivation($\Delta V_{1/2}$) generated by CaM in WT and mutated $Na_V1.8$ channels. $\Delta V_{1/2}$ are assessed from (***J***) (*$P < 0.05$). (For interpretation of the references to colour in this figure legend, the reader is referred to the Web version of this article.)